D-RING MODIFICATIONS OF THE PHYLLANTHUSMIN CLASS OF ARYLNAPHTHALENE LIGNAN NATURAL PRODUCTS

DISSERTATION

Presented in Partial Fulfillment of the Requirements for the Undergraduate Graduation with Honors Research Distinction at The Ohio State University

By

Aimee Ho

Bachelors of Science in Pharmaceutical Sciences

College of Pharmacy

The Ohio State University

2019

Dissertation Committee:

Professor James R. Fuchs, Advisor

Professor Mark Mitton-Fry

Professor Terry Elton

Abstract

Natural products isolated from plants of the Phyllanthus genus, specifically members of the arylnaphthalene subclass of lignan lactones, show promise as a potential treatment option for ovarian cancer. These compounds are worth examining further because several structurally related synthetic analogues have displayed highly potent cytotoxic activities against ovarian cancer cell lines in the nanomolar range. Our lead compound, PHY34, exerts its cytotoxic effects by inhibiting autophagy in ovarian cancer cells which is followed by apoptotic cell death. Potent experimental agents with attractive mechanisms of action, including autophagy modulators, are needed to continue to fight cancer, potentially overcoming the problem of chemoresistance and increasing the chances of survival for patients.

In order to further assess and obtain structure-activity relationship data for this class of compounds, several new analogues were synthesized by modifying the D-ring on the diphyllin core of the phyllanthusmins. The diphyllin precursors, representing the core ring system, were synthesized using a five-step method with 3,4-dimethoxybenzaldehyde as the precursor. At that stage, the sugar moiety could then put on at the C7 position to complete the synthesis of the derivatives. A total of six analogues with D-ring modifications were made, and characterization data was collected for both the diester and diphyllin precursors to confirm the structural assignments. This included collection of both proton and carbon NMR spectra for each compound for a total of twelve proton NMR spectras and twelve carbon NMR spectras as well as the determination of their accurate masses using mass spectrometry. Biological data for four of these compounds were also obtained to assess their potency against two ovarian cancer cell lines.

Dedication

I would like to dedicate this thesis to my friends, family, and mentors who have encouraged and supported me throughout my undergraduate career.

Acknowledgements

I would like to acknowledge the members of the Fuchs Group for allowing me to develop as a student and researcher with their invaluable guidance and insight.

I would like to acknowledge the funding that made this project possible:

National Institutes of Health (NIH) 2P01 CA125066-10 program project.

I would also like to acknowledge the collaborators:

The Kinghorn Group (isolation and elucidation) and the Burdette Group (biological activity).

Table of Contents

List of Figures

Chapter 1: Ovarian Cancer

1.1 Cancer Disease State

Cancer is a disease characterized by abnormal cell growth which can then spread to other organs and areas of the body in a process known as metastasis.[1] In normal healthy cells of the body, the cell cycle, the process in which cells replicate DNA and divide into two identical daughter cells, is tightly regulated by checkpoints in the G1 phase, the G2 phase, and the metaphase. Dysfunctions in the checkpoints can cause premature cell death or cell cycle reprogramming which can eventually lead to tumor growth.[2] These tumors then become classified as malignant when they start to spread to other parts of the body.

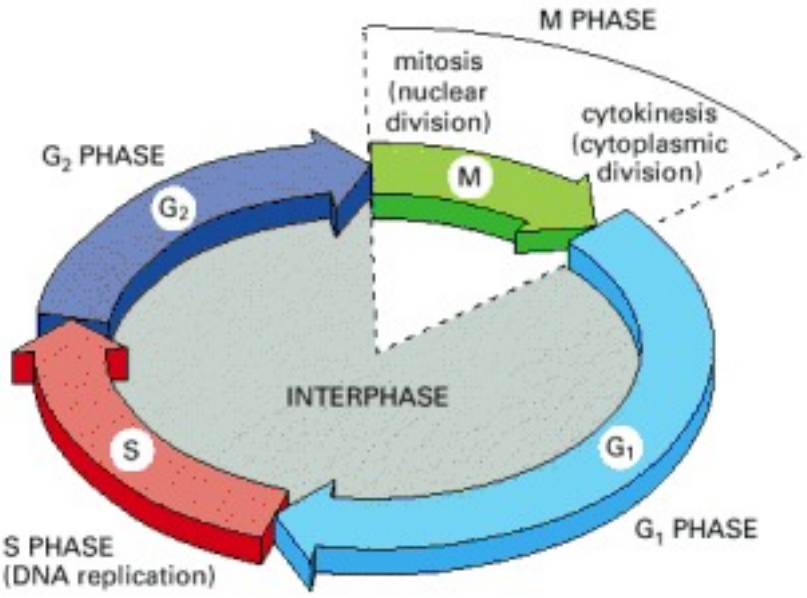

Figure 1.1 Cell Cycle
Source: https://www.ncbi.nlm.nih.gov/books/NBK26869/

The causes of cancer include both genetic and external factors. According to the National Cancer Institute at the National Institutes of Health, inherited genetic mutations are a significant factor in about 5 to 10 percent of all cancers.[3] External factors, known as carcinogens, may

include physical, chemical, and biological agents or exposures. For example, high-energy radiation such as x-rays and gamma rays are physical carcinogens that can cause damage to DNA and disrupt the normal processes of the cell cycle. Chemical carcinogens such as formaldehyde and those found in tobacco smoke can also lead to DNA damage. Certain infectious agents like human papillomavirus and hepatitis B virus are biological carcinogens that can cause cancer through a variety of factors including disrupting the cell cycle, weakening the immune system, and causing chronic inflammation.[4]

There are many different types of cancer, and they are named based on where the cancer originated. Ovarian cancer first develops in the ovaries of the female reproductive system or in the surrounding fallopian tubes and peritoneum lining.[1] All women have a risk of developing ovarian cancer, but there are also several factors that could increase the risk including having a mutation in the *BRCA1*or *BRCA2* gene, taking estrogen by itself for more than ten years, and having close family members that have had ovarian cancer.[1] Ovarian cancer is assigned a stage from I to IV depending on the size of the tumor, the spread to nearby lymph nodes, and the spread to distant sites with stage IV being the most severe.[4] The symptoms of ovarian cancer include vaginal bleeding, abdominal pain, bloating, and trouble eating.[3] These symptoms do not seem serious in themselves, but, if left untreated, ovarian cancer can spread to other organs such as the spleen or liver and shut down important biological processes which can lead to death.

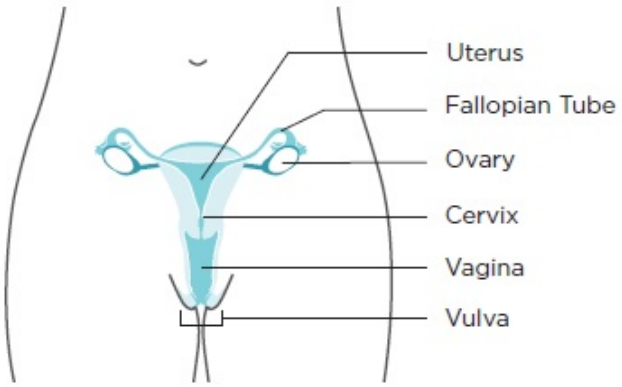

Figure 1.2 Female Reproductive System
Source: https://www.cdc.gov/cancer/ovarian/basic_info/index.htm/

1.2 Demographics

Rates of new cases of cancer in the United States according to data from the Centers for Disease Control and Prevention (CDC) is detailed in Figure 1.3 and 1.4. They show that 1,633,390 new cases of cancer were reported in 2015, and 595,919 people died of cancer. Of those reported cases, 21,429 were new cases of ovarian cancer, and 13,920 women died of ovarian cancer.[6] The five-year relative survival rate for all cancer patients is 65.6%, but that percentage drops to 46.1% for patients with ovarian cancer specifically.[6]

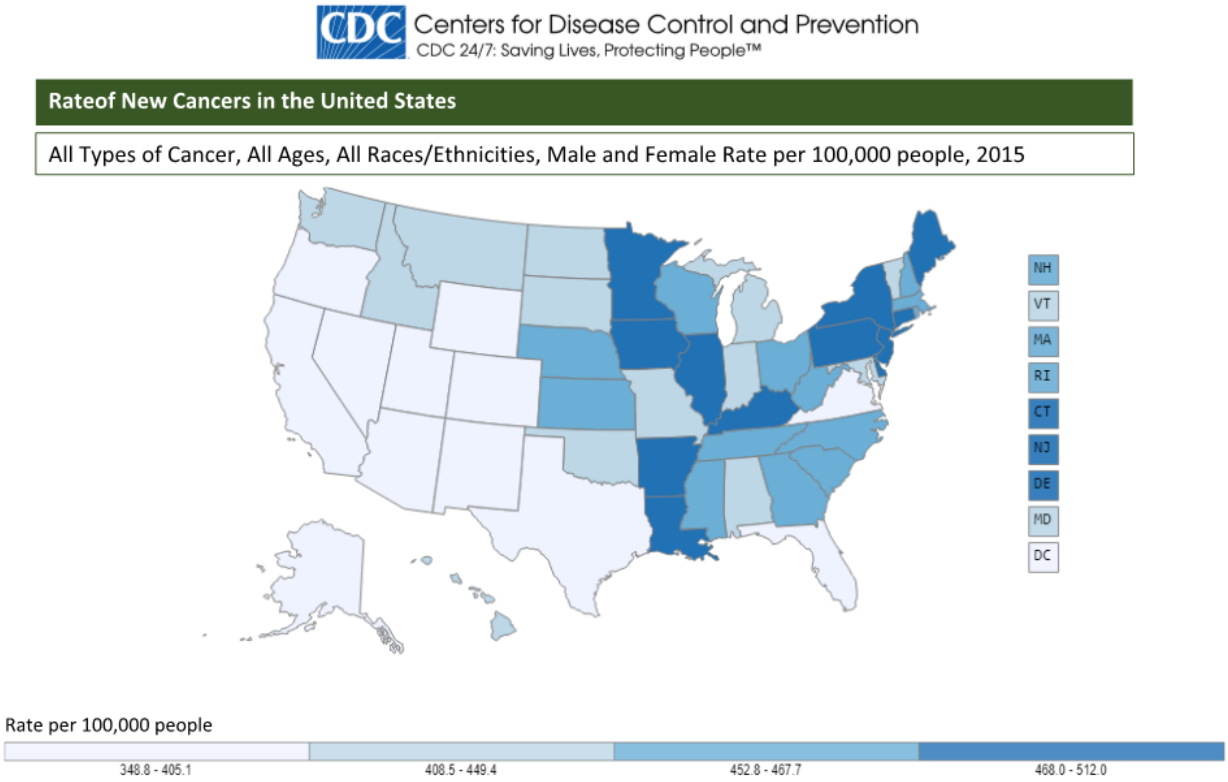

Figure 1.3 Rates of new cases of cancer in the U.S.
Source: https://gis.cdc.gov/Cancer/USCS/DataViz.html

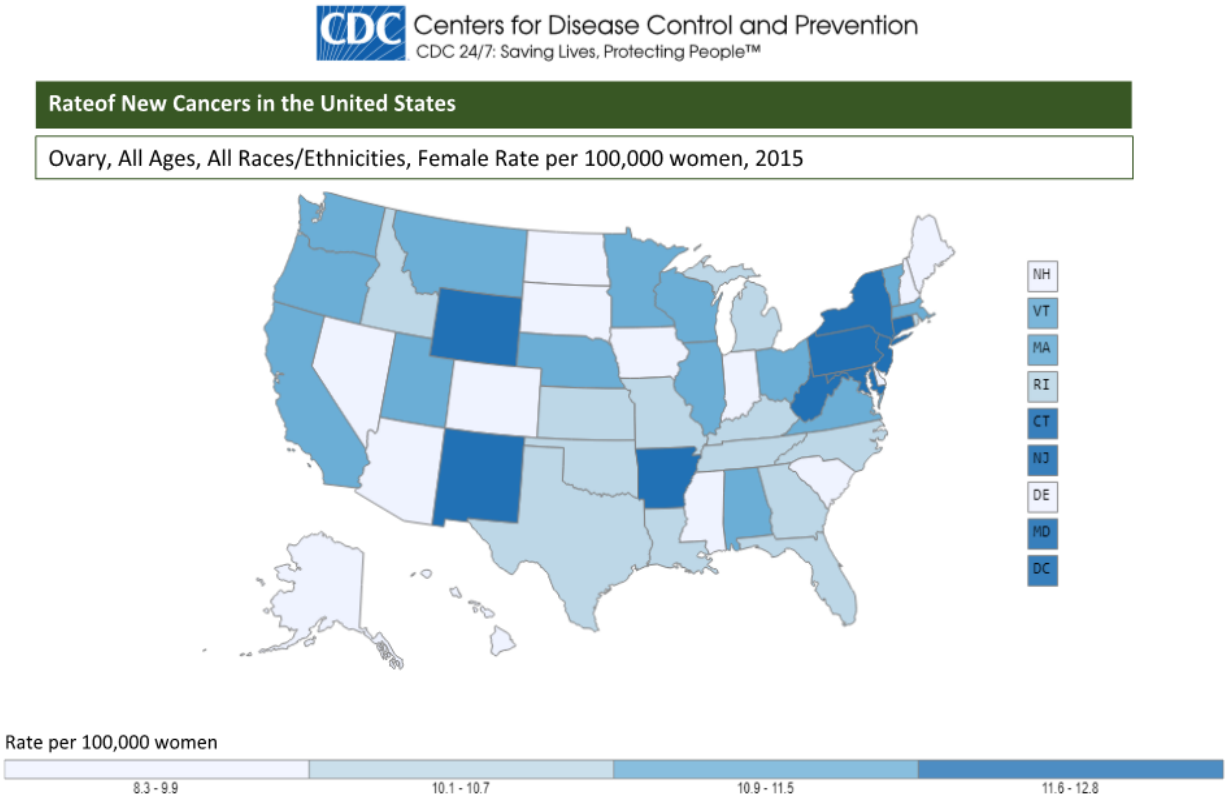

Figure 1.4 Rates of new cases of ovarian cancer in the U.S.
Source: https://gis.cdc.gov/Cancer/USCS/DataViz.html

The World Health Organization (WHO) claims that 30-50% of cancer deaths could be prevented if patients modified certain aspects of their lifestyles such as maintaining a healthy body weight, exercising regularly, avoiding tobacco smoke, and reducing alcohol consumption.[7] Nonetheless, cancer continues to claim millions of lives globally. WHO has identified cancer as the world's second leading cause of death and has estimated that it is the cause of 9.6 million deaths in 2018.[7] As more and more cases arise each year, is has become necessary to look for new ways to combat this serious problem.

1.3 Current Chemotherapy Drugs for Ovarian Cancer

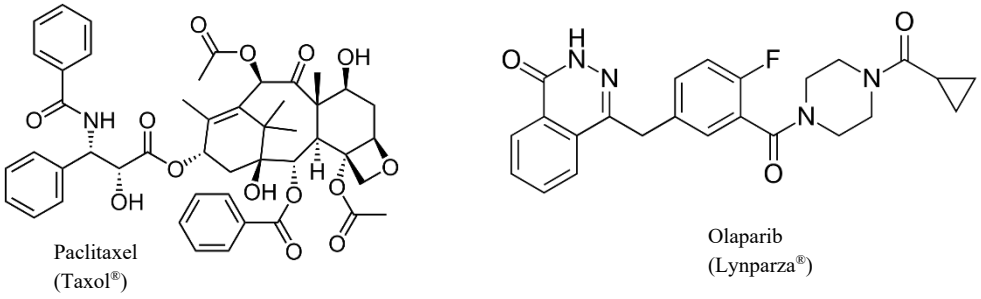

Figure 1.5. Some current widely used chemotherapeutics for the treatment of ovarian cancer.[8]

The primary therapeutic approach for patients with advanced cancer progression during their initial diagnosis is cytoreductive surgery followed by a combination of platinum-based and taxane-based chemotherapy. First-line treatment is initially effective with many patients who achieve complete remission, but up to 80% of these patients also experience relapse due to rapidly developed chemoresistance.[8] Maintenance therapy with drugs such as bevacizumab, a recombinant monoclonal antibody with antiangiogenic properties, and olaparib, a PARP, poly ADP ribose polymerase, inhibitor, have been used in clinical trials in order to assess their effectiveness against recurrent ovarian cancer. However, the results have shown that cumulative toxicity is a major issue with maintenance therapy, and it does not provide clinically significant increases in survival benefits.[9]

There are a great number of anticancer drugs because of the wide variety of biological targets that can be exploited in cancer cells and their life cycles as shown in **Figure 1.6**. Paclitaxel, shown in **Figure 1.5**, **is** a member of the taxane class of molecules. It exerts its antitumor properties by stabilizing microtubule polymers in cancer cells which subsequently arrests cells in the metaphase and prevents them from further replicating.[10] Olaparib has a different mechanism of action in that it inhibits PARP enzymes, proteins that play a key role in

DNA repair.[11] As patients continue to develop chemoresistance towards the current approved drugs on the market, there is an urgent need to develop new drugs with novel mechanisms of action in order to increase patients' chances of survival.

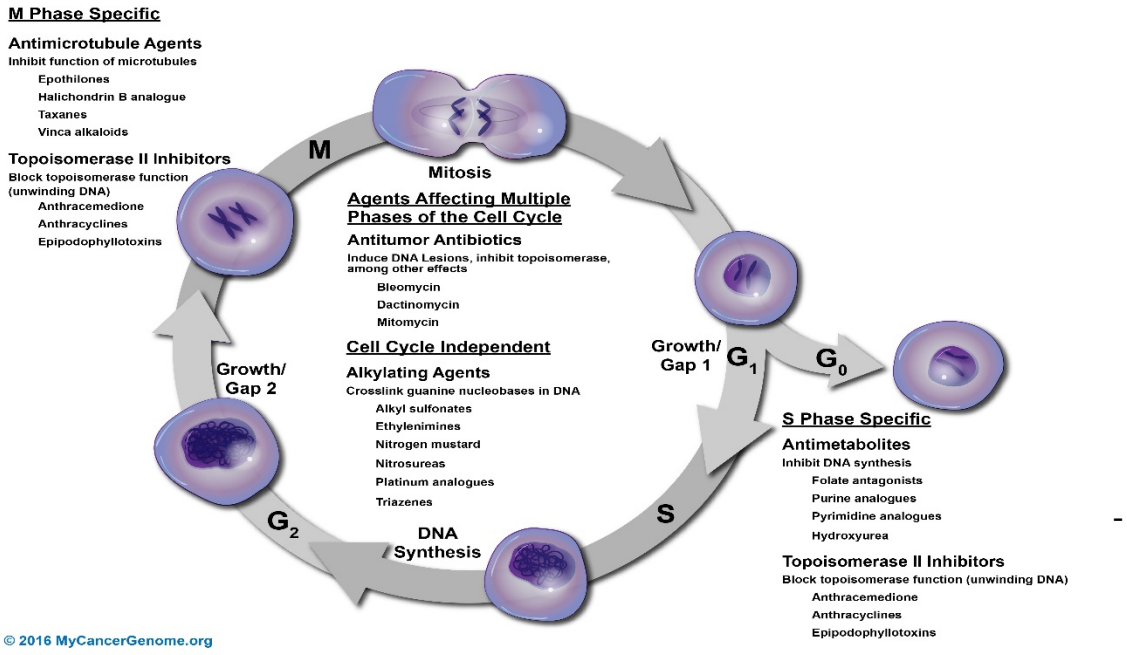

Figure 1.6 Cytotoxic chemotherapy mechanisms of action[12]

Chapter 2: Antiproliferative Activity of the Phyllanthusmin Class of Arylnaphthalene Lignan Natural Products

Discoveries in natural products have led to breakthroughs in cancer chemotherapy. The arylnaphthalene subclass of lignan lactones represents a relatively recently discovered chemotype that has been found to possess potent cytotoxicity toward human cancer cell lines. For example, both justicidin A (Figure 2.1), a methylated diphyllin derivative, and acutissimalignan A, a diphyllin methylated arabinoside derivative, exhibited cytotoxicity towards cancer cell lines in the nanogram per milliliter range.[13,14]

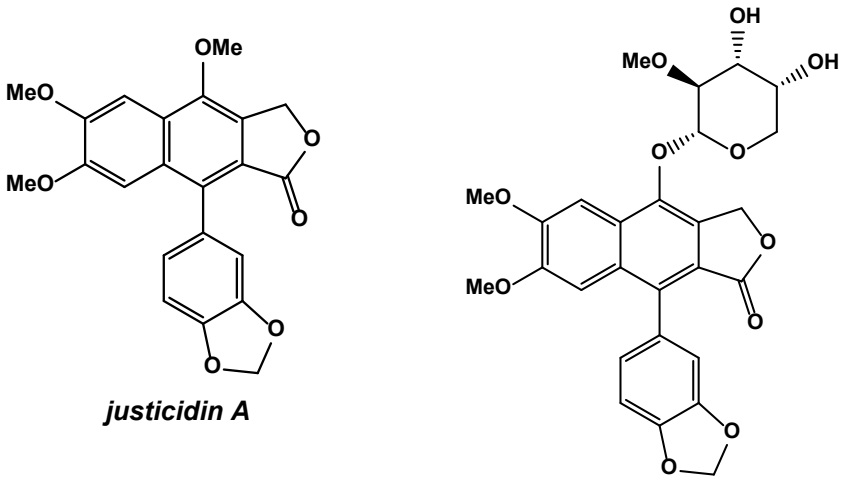

Figure 2.1. Two examples of cytotoxic arylnaphthalene lignan lactones

The phyllanthusmins, which are also members of the arylnaphthalene subclass of lignan lactones, are natural products isolated from plants from the *Phyllanthus* genus. Species from this genus have been utilized in traditional Asian medicine for their anticancer, antiviral, and insecticidal properties.[15] *Phyllanthus poilanei* samples, shown in **Figure 2.2**, were collected in South

Figure 2.2 *Phyllanthus poilanei*
Photo by D.D. Soejarto

Vietnam by Dr. Doel Soejarto between 2004 and 2011 as a part of a P01 grant. Dr. A. Douglas Kinghorn (Division of Medicinal Chemistry & Pharmacognosy, OSU College of Pharmacy) and his lab were then able to isolate two novel (**1** and **2** in **Figure 2.3**) and four known (**3-6** in **Figure 2.3**) arylnaphthalene lignan lactones from the chloroform-soluble extract using a bioassay guided fractionation approach against HT-29 colon carcinoma cells. As a part of these studies, diphyllin (**8**) and the semisynthetic derivative (**7**) were also made and evaluated for their activity against HT-29 human colon cancer lines.[16] This data is shown in **Figure 2.4**. From a structural perspective, all of the isolated compounds in this series possess the diphyllin core ring system, although phyllanthusmin A (**6**) lacks a methyl group at the C4 position. In addition, compounds **1**-**5** have a sugar moiety attached to the C7 phenolic oxygen atom of diphyllin. For the phyllanthusmins B-E (**1**-**4**) this is a substituted arabinose ring, while for cleistanthin B (**5**), this is a glucose ring.

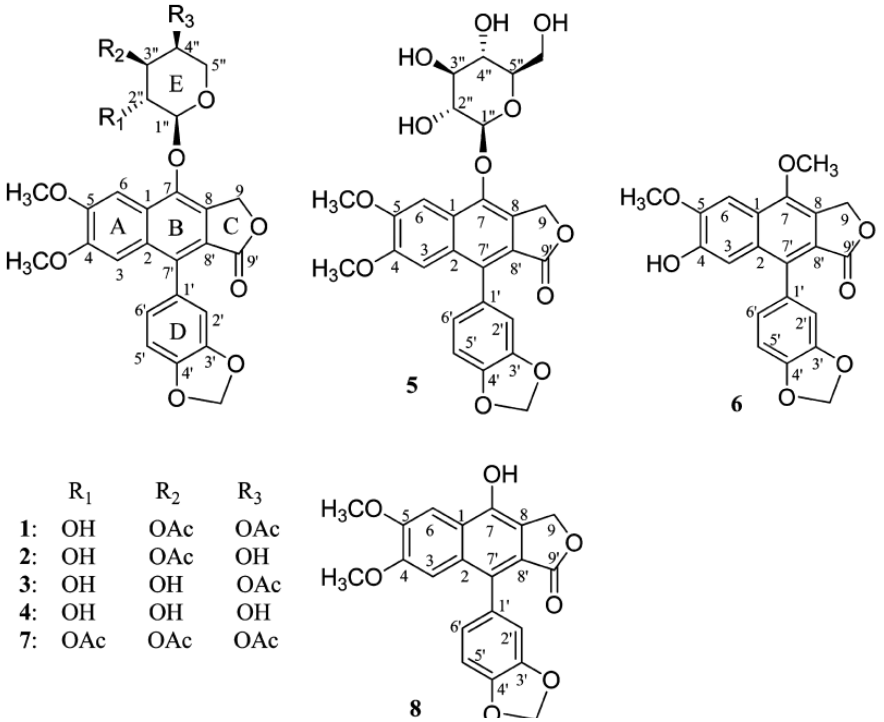

Figure 2.3 Compounds isolated and derived from chloroform-soluble extract of *Phyllanthus poilanei*[16]

Compound	HT-29
1	0.17
2	1.8
3	1.8
4	3.2
5	12.2
6	>10
7	0.11
8	7.6
Paclitaxel*	0.001

Figure 2.4 Cytotoxicity of compounds isolated and derived from chloroform-soluble extract of *Phyllanthus poilanei* toward H-29 cells. * FDA approved anticancer drug paclitaxel was used as a positive control.[16]

Previous published studies pertaining to other arylnaphthalene compounds similar in structure to the phyllanthusmins have revealed the importance of the glycosidic sugar moiety to the antiproliferative properties of this class of lignans.[17,18,19] Diphyllin glycosides such as phyllanthusmins B-E[16] and D11[19] have been shown to possess more potent *in vitro* activity against cancer cell lines than their aglycone, diphyllin, alone. Based on this knowledge of the influence of the sugar moiety for potent antiproliferative activity, the graduate students in the Fuchs lab have previously synthesized a number of different glycone analogues as well as C-ring lactone analogues to further explore the structure-activity relationships of the phyllanthusmins. The results they gathered led to the conclusion that substituted (acetylated or methylated) hydroxy groups on the sugar moieties, as opposed to the unsubstituted alcohols, and the lactone carbonyl on the aglycone are needed for more potent biological activity.[20] A modified galactose moiety, PHY34, is our most promising current lead compound with an IC_{50} values of 4.2 nM against OVCAR-3

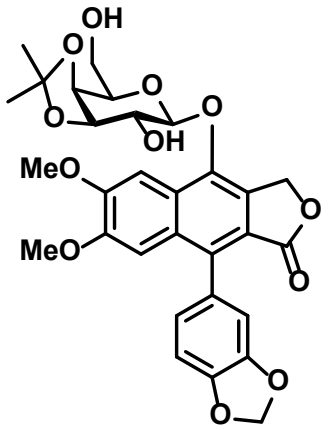

Figure 2.5 Lead compound PHY34

cell lines and 4.0 nM against OVCAR-8 cell lines.[21] In addition to *in vitro* antiproliferative activities, this compound has also been studied in both *in vivo* hollow fiber and xenograft studies in the lab of Dr. Joanna Burdette (Department of Medicinal Chemistry & Pharmacognosy, UIC College of Pharmacy). For the xenograft study, OVCAR8-RFP, fluorescently-labeled OVCAR8 cells, were xenografted intraperitoneally into female mice and monitored by IVIS imaging. Once treatment was initiated, the mice were dosed three times a week for three weeks with PHY34 (0.75 mg/kg) or paclitaxel (5 mg/kg), the positive control. At the completion of the study it was shown that PHY34 significantly decreased tumor burden as compared with the vehicle with no gross toxicities observed as shown in **Figure 2.6**.[21]

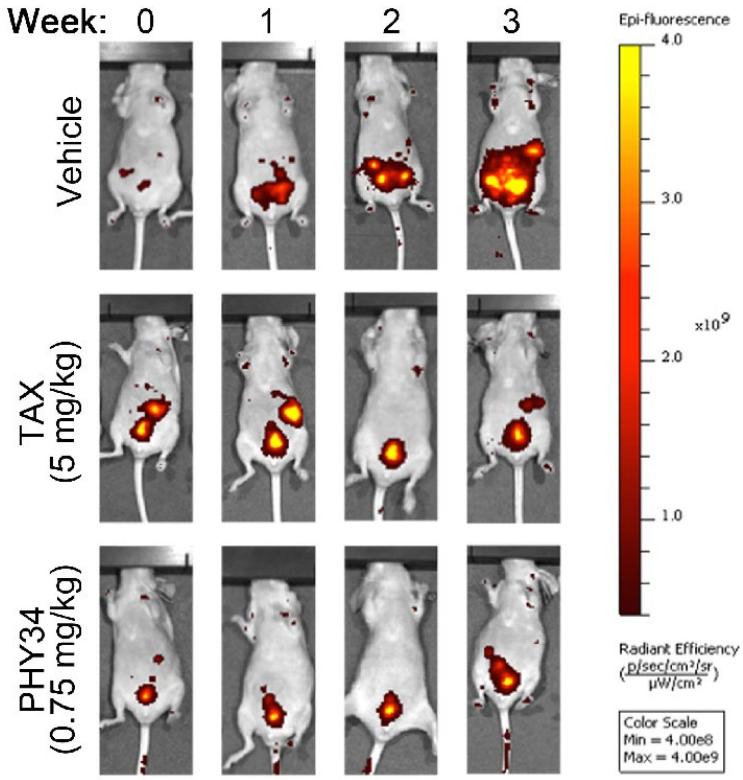

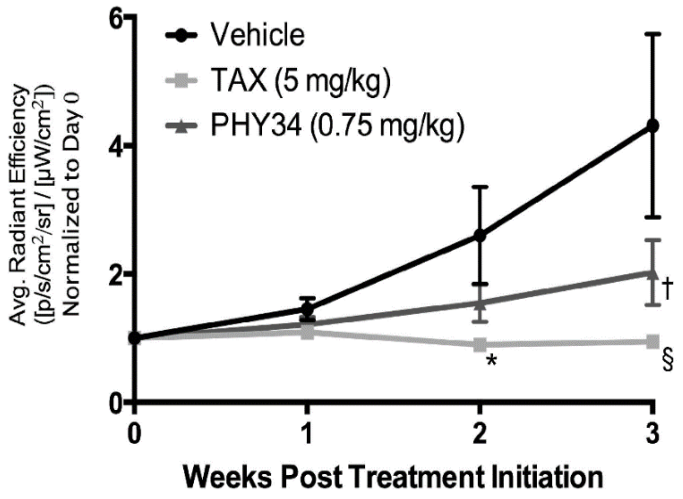

Figure 2.6 Biological activity of PHY34 in mice as compared to paclitaxel[21]

Subsequent studies by the Burdette lab have shown that the proposed mechanism of action for PHY34 is that it acts as a late-stage autophagy inhibitor which is followed by apoptotic cell death.[21] This is significant because biomarkers for autophagy, such as Beclin1 and LC3A, have been shown to correlate with poor prognosis in certain ovarian cancers which demonstrates the potential influence of the autophagic pathway in ovarian cancer.[22,23] Combination treatment with autophagy inhibitors may also help overcome the problem of disease recurrence and chemoresistance in patients with ovarian cancer and increase the chances of survival. The desire to further explore the structure-activity relationship of the phyllanthusmins by modifying different parts of the compound other than the sugar moiety led to the subsequent synthesis of a number of D-ring analogues.

Chapter 3: Synthesis and D-Ring Modifications on Diphyllin Core of Phyllanthusmins

The phyllanthusmins provide a unique opportunity to carry out relatively exhaustive SAR studies on a somewhat complex natural product scaffold. This is due in part to the fact that elegant synthetic approaches to diphyllin, the aglycone structure, have previously been established[5]. When this project was initiated in the Fuchs lab, a search of the existing methodology showed that diphyllin could be readily accessed from simple, commercially available starting materials. Subsequent glycosylation of the phenolic oxygen of diphyllin could then lead to the phyllanthusmins and a potentially wide range of substituted analogues.

3.1 Synthetic Approach

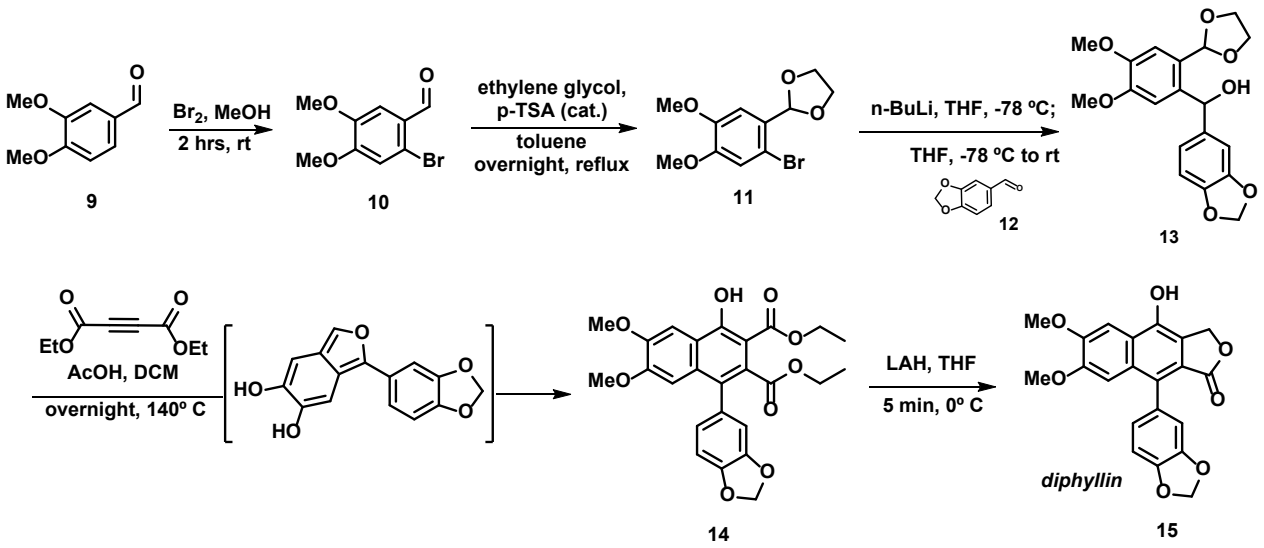

Figure 3.1 Charlton reaction scheme with modification to last step to synthesize diphyllin[5,20]

As connecting the sugar moiety to the diphyllin core via a glycosidic linkage was expected to be a relatively straightforward step, the synthesis of phyllanthusmin analogues depended on the ability to generate sufficient quantities of diphyllin in an efficient manner. Using the reaction scheme of Charlton and coworkers[5], with a slight modification to the final

reduction step of the diester to the diphyllin, our lab has been able to produce diphyllin in gram scale quantities. The use of 3,4-dimethoxybenzaldehyde as the starting material allowed the complete synthesis of diphyllin in just five steps. First, 3,4-dimethoxybenzaldehyde (**9**) was brominated through electrophilic aromatic substitution to afford compound **10**. An acetal protection step was then performed using ethylene glycol and *p*-toluenesulfonic acid as the catalyst to prevent the *n*-butyllithium from reacting with the ketone in the subsequent step. Compound **11** was then subjected to a lithium-halogen exchange before the slow addition of piperonal (**12**). The intermediate (**13**) was then immediately subjected to a Diels-Alder reaction using acetic acid and diethyl acetylenedicarboxylate. A column chromatography using dry loading was performed at this step to obtain the pure diester intermediate (**14**). The final reduction step of the diester to afford diphyllin (**15**) was performed by adding four equivalents of portion-wise lithium aluminum hydride which differs from the reported sodium borohydride reduction conditions of Charlton and coworkers. The crude product was finally triturated with methanol to cleanly provide diphyllin.

With the synthesis of diphyllin in hand, we were interested in derivatizing diphyllin to explore the role of structural changes, specifically with regard to the substitution of the aromatic rings, on biological activity. As mentioned previously, SAR studies in our lab on the phyllanthusmins had been limited primarily to modifications of the sugar moiety appended to diphyllin. Little was known about the role that the aromatic substituents play in the activity of these compounds. Based on the synthetic route employed for the synthesis of diphyllin, we felt that the substituents of the D-ring could be varied effectively through replacement of piperonal in Figure 3.1 with other appropriately substituted aromatic aldehydes.

The most significant challenge in the application of this strategy to the synthesis of new analogues was the alkylation/Diels-Alder sequence. In this case, the halogen-metal exchange reaction with the bromobenzene derivative is highly water sensitive. Based on the fact that the newly generated anion can be quenched in the presence of even trace quantities of moisture, the reaction is carried out under anhydrous conditions. Furthermore, the addition into the aldehyde group leads to the formation of a relatively unstable alcohol. This alcohol cannot be chromatographed and is instead taken forward directly to the next step without purification. This requires the alkylation reaction to be reasonably clean. The relative conversion of this reaction is therefore monitored by ^{1}H NMR after workup.

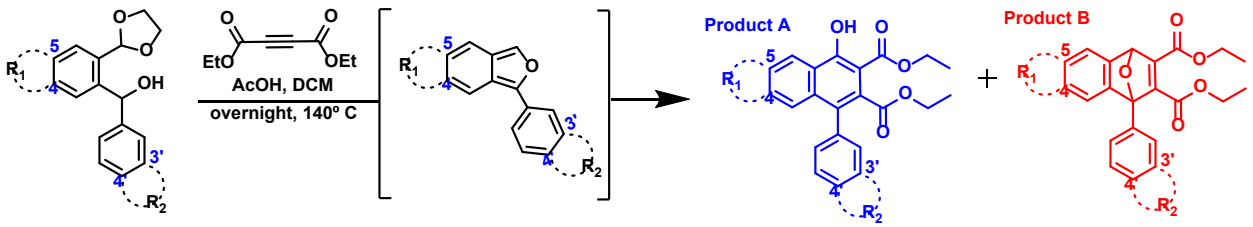

Figure 3.2 Initial Diels-Alder reaction conditions lead to formation of two products

The subsequent step in this sequence is the Diels-Alder reaction in the presence of diethyl acetylenedicarboxylate and acetic acid. In preliminary experiments by Ms. Bernadette Latimer, a past undergraduate researcher in the Fuchs lab, it was observed that the desired aromatic product, possessing the newly formed aromatic benzene ring, was only formed in low yield. Instead, the major product of this reaction was observed to be the bridged bicyclic intermediate shown in **Figure 3.2** (product B). This bridged bicyclic intermediate is the compound that is formed upon initial cycloaddition reaction of the alkyne with the furan intermediate. Under typical reaction conditions, as in our synthesis of diphyllin, this bridged bicyclic system undergoes a ring opening

and elimination reaction to generate the benzene ring. As compared to our synthesis of diphyllin, however, on small scale this cycloaddition reaction appears to "stall" prior to the ring opening. Subsequent treatment of product B with acid in could promote formation of the aromatic ring [26], although this was not very efficient. Based on these results, the reaction conditions were re-examined and it was found that careful control of the concentration and equivalents of acetic acid were critical for the direct formation of the naphthalene system. These analogues could then be directed converted to the corresponding lactones through application of the LAH reduction. In this way, a series of six D-ring analogues, refer to **Figure 3.3**, were synthesized. Interestingly, while utilizing these conditions for the preparation of the *p*-anisaldehyde, *m*-anisaldehyde, and 2-(benzyloxy)-1,3-dimethoxybenzene D-ring analogues, an additional spot showed up on thin-layer chromatography after the Diels-Alder reaction. Spectroscopy data revealed that it was most likely excess aldehyde. An additional purification step was needed and performed using dimethylformamide and sodium bisulfite before column chromatography.[25] This result suggests that the Diels-Alder reaction tolerates additional impurities present during the course of the reaction.

With the diphyllin analogues in hand, these compounds were analyzed using a combination of spectroscopic techniques. Most notably, ^{1}H and ^{13}C NMR spectra were obtained for all of the compounds in order to confirm the assigned structures. Experimental procedures and NMR spectroscopic data are included in Chapter 4 and the Appendix of this document, respectively. Accurate mass data were also obtained for these compounds through mass spectrometry.

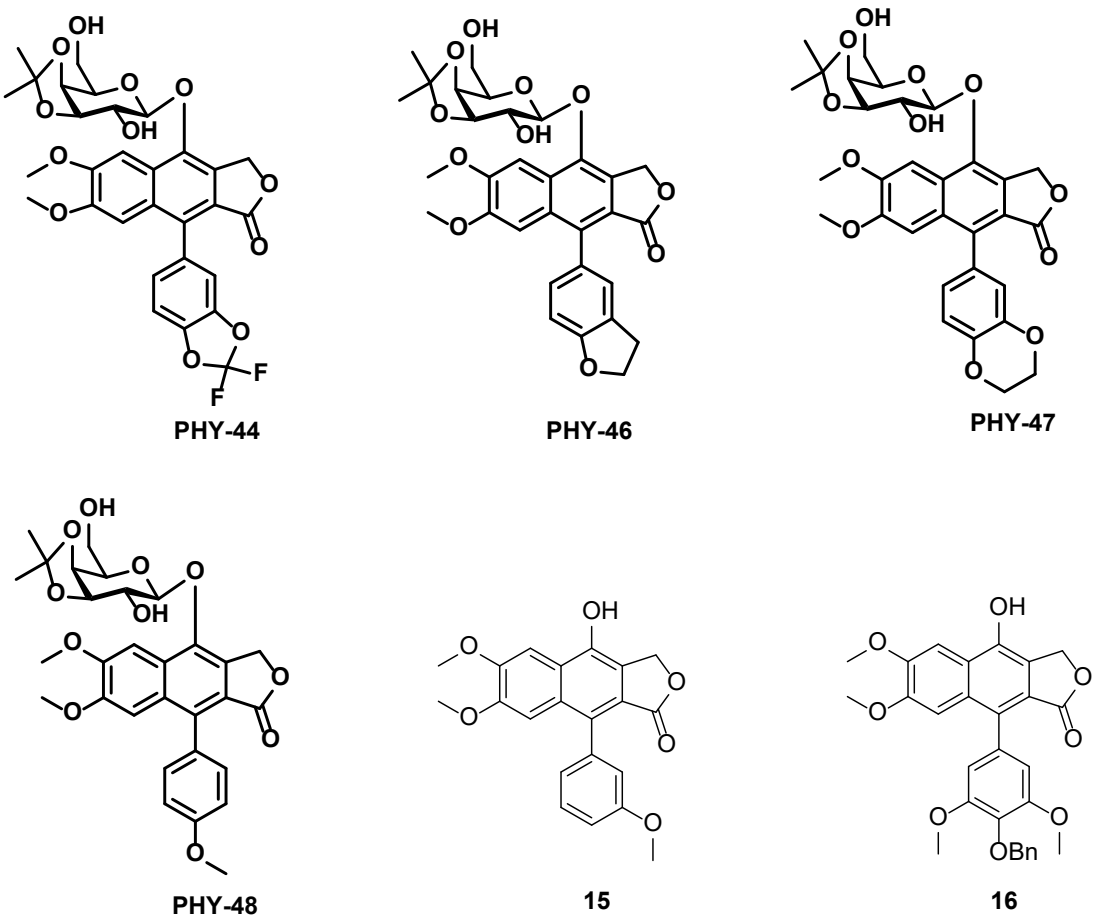

Figure 3.3 Final D-Ring analogues synthesized

Four of the compounds generated in this study were then passed on to Mr. Andrew Huntsman in the Fuchs lab for conversion to the glycosides affording PHY-44, PHY-46, PHY-47, and PHY-48. These glycosides possess the same sugar moiety as PHY-34, namely a galactose ring with a dimethyl acetal spanning the oxygen atoms attached to the C3 and C4 positions.

3.2 Biological Studies

Compound	OVCAR-3	OVCAR-8
PHY-34	0.004	0.004
PHY-44	0.33	0.0046
PHY-46	0.93	0.0063
PHY-47	0.093	0.10
PHY-48	0.062	0.027
Paclitaxel*	7.88	8.05
Etoposide*	2.89	8.94

Figure 3.3 PHY-34 and D-ring analogues and corresponding antiproliferative data in OVCAR-3 and OVCAR-8 cell lines expressed as GI_{50} values in µM. *FDA approved anticancer drugs paclitaxel and etoposide were used as reference standards in this experiment.

The four final D-ring derivatives with the glycoside of PHY-34, the optimized modified galactose moiety, on the C7 position of the diphyllin core were submitted to Dr. Burdette's lab at the University of Illinois at Chicago for biological testing. The results show that PHY-44 and PHY-46 exhibited the greatest potencies against the OVCAR-8 cell line while PHY-47 and PHY-48 exhibited higher potencies against the OVCAR-3 cell line than the rest of the compounds. Interestingly, none of the compounds demonstrated greater than or even equal to the potency of PHY-34 against ovarian cancer cell lines. In HT-29 cells (data not shown), however, both PHY-44 and PHY-48 were equal to or slightly more potent (~ 2 fold) than PHY-34. Overall, this data indicates that the D-ring is very important for the binding of these compounds to their biological target(s) and appears to be highly engineered by nature to fit the binding site. It is not surprising that PHY-44 shows reasonable potency based on the fact that the hydrogen atoms of the methylenedioxy functionality of PHY-34 have been replaced with bioisosteric fluorine atoms. The drop in potency for PHY-46 in the OVCAR-3 cell line indicates the

importance of the second oxygen atom in that ring, although PHY-48, which is acyclic and lacks the second oxygen atom still retains good potency. One other interesting observation with these compounds is that PHY-44 and PHY-46 show significant differences in potencies for the two ovarian cancer cell lines (71-fold and 147-fold differences, respectively). These differences were seen with many other phyllanthusmin analogues as well, but analogues that closely resemble PHY-34 typically showed similar potencies against both of these cell lines. This fact may point to the presence of multiple targets for these compounds that are highly structurally specific.

Chapter 4: Experimentals

Note: Analogues **14a**, **14b**, and **14c** were first synthesized by Ms. Bernadette Latimer, a past undergraduate in the Fuchs lab. I remade these compounds and collected the characterization data.

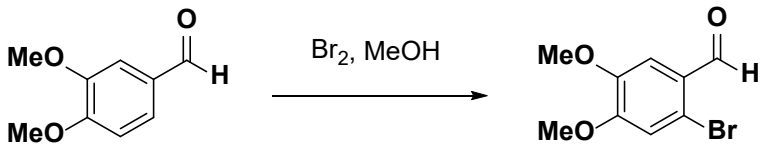

2-bromo-4,5-dimethoxybenzaldehyde. To a solution of 3,4-dimethoxybenzaldehyde in methanol (1.00 equiv.) was treated with dropwise addition of bromine (1.05 equiv.) and stirred at 23 °C for 4 hours. Following completion, the methanol was removed under reduced pressure. The solid was then dissolved in DCM and washed with $Na_2S_2O_3$ then brine. The organic layer was dried over anhydrous sodium sulfate and concentrated under reduced pressure to afford an orange solid. Spectroscopic data were consist with previously published data.[5]

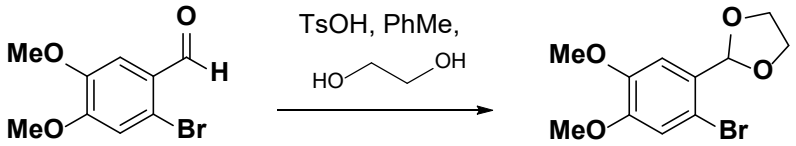

2-(2-bromo-4,5-dimethoxyphenyl)-1,3-dioxalane. To a suspension of crude 2-bromo-4,5-dimethoxybenzaldehyde in toluene (1.00 equiv.) was added ethylene glycol (4.00 equiv.) and *p*-toluenesulfonic acid (0.20 equiv.). Using a Dean-Stark apparatus filled with toluene, the reaction was refluxed overnight. After cooling to 23 °C, the toluene was removed under reduced pressure. The reaction mixture was then dissolved with EtOAc and washed with sodium bicarbonate, water, and then brine. The organic layer was dried over anhydrous sodium sulfate and

concentrated under reduced pressure. The crude product was purified via deactivated silica gel column chromatography (EtOAc-hexanes, 16:84 → 25:75) to afford 2-(2-bromo-4,5-dimethoxyphenyl)-1,3-dioxalane as an off-white solid. Spectroscopy data was consist with previously published data.[1]

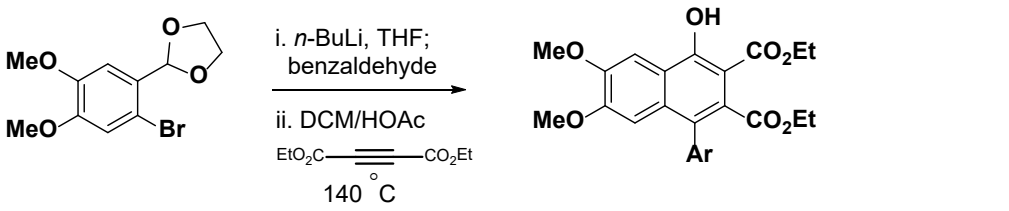

14a Ar = 2,2-difluorobenzo[d][1,3]dioxole
14b Ar = 2,3-dihydrobenzofuran
14c Ar = 2,3-dihydrobenzo[b][1,4]dioxine
14d Ar = 4-methoxyphenyl
14e Ar = 3-methoxyphenyl
14f Ar = 2-(benzyloxy)-1,3-dimethoxybenzene

General procedure for arylnaphthalene diester formation:

To a solution of the acetal in dry THF (0.98 equiv.) was added *n*-BuLi (2.00 equiv.) and cooled to -78 °C. After stirring for 20 minutes, a solution of a substituted benzaldehyde in THF (1.00 equiv.) was added to the reaction mixture slowly. The reaction was then stirred at -78 °C for an additional 30 minutes before slowly letting it warm to 23 °C. After stirring at 23 °C for an additional 2 hours, the reaction was quenched with water, and the aqueous layer was extracted with EtOAc. The combined organic layers were washed with water and then brine. The organic layer was dried over anhydrous sodium sulfate and concentrated under reduced pressure to afford a yellow syrup. To a solution of the crude product in DCM (1.00 equiv.) was then added AcOH (1.00 equiv.) and diethyl acetylenedicarboxylate (1.00 equiv.). The reaction was stirred at 140 °C under reflux overnight. After cooling to 23 °C, the aqueous layer was extracted with DCM. The combined organic layers were washed with water, sodium bicarbonate, and then brine. The

resulting solution was then dried over anhydrous sodium sulfate and concentrated under reduced pressure. The crude product was purified via silica gel column chromatography (EtOAc-hexanes, 10:90) to obtain the corresponding naphthalenes **14a-14f**.

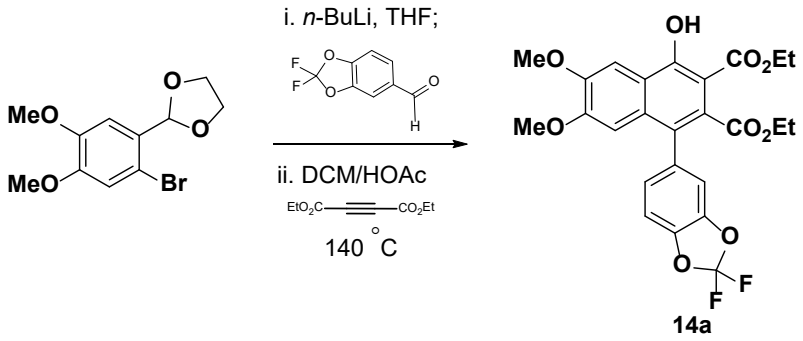

Difluorobenzodioxole 14a. Using 2-(2-bromo-4,5-dimethoxyphenyl)-1,3-dioxalane as the starting material (0.300 g, 1.04 mmol) and 2,2-difluorobenzo[d][1,3]dioxole-5-carbaldehyde as the aldehyde (0.193 g, 1.04 mmol), the above general procedure afforded compound **14a** (0.189 g, 0.375 mmol, 37%) as a yellow oil: ^{1}H NMR (300 MHz, $CDCl_3$) δ 12.47 (s, 1H), 7.75 (s, 1H), 7.16 – 7.02 (m, 3H), 6.61 (s, 1H), 4.41 (q, J = 7.1 Hz, 2H), 4.05 (s, 3H), 4.17 – 3.93 (m, 2H), 3.76 (s, 3H), 1.36 (t, J = 7.1 Hz, 3H), 1.02 (t, J = 7.1 Hz, 3H); ^{13}C NMR (400 MHz, $CDCl_3$) δ 170.18, 168.51, 159.95, 152.67, 149.87, 143.45, 143.30, 133.10, 131.73, 129.34, 126.43, 126.11, 119.89, 112.40, 109.03, 105.28, 102.96, 101.17, 62.11, 60.98, 56.13, 55.87, 29.70, 13.89, 13.71; HRMS-ESI calcd for $C_{25}H_{22}F_2O_9$ $(M+Na)^+$ 527.11259, found 527.11241.

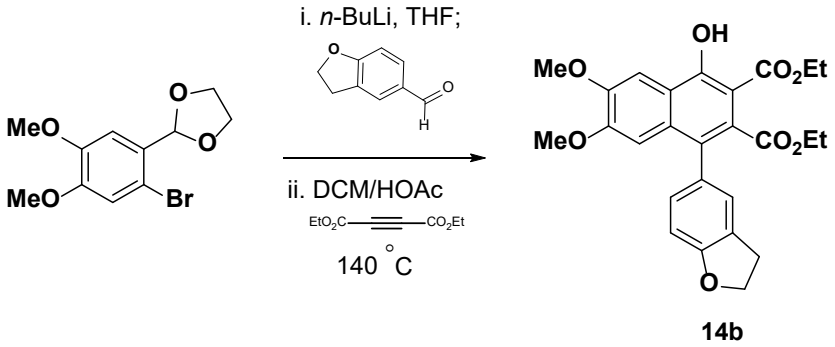

Tetrahydrofuran 14b. Using 2-(2-bromo-4,5-dimethoxyphenyl)-1,3-dioxalane as the starting material (0.300 g, 1.040 mmol) and 2,3-dihydrobenzofuran-5-carbaldehyde as the aldehyde (0.153 g, 1.038 mmol), the above general procedure afforded compound **14b** (0.082 g, 0.176 mmol, 17% yield) as a yellow oil: ^{1}H NMR (300 MHz, $CDCl_3$) δ 12.44 (s, 1H), 7.75 (s, 1H), 7.17 – 6.81 (m, 3H), 6.76 (s, 1H), 4.65 (td, *J* = 8.8, 2.6 Hz, 2H), 4.41 (q, *J* = 7.1 Hz, 2H), 4.06 (s, 3H), 4.01-3.96 (m, 2H), 3.76 (s, 3H), 3.27 (t, *J* = 8.5 Hz, 2H), 1.37 (t, *J* = 7.1 Hz, 3H), 1.03 (t, *J* = 7.1 Hz, 3H); ^{13}C NMR (400 MHz, $CDCl_3$) δ 170.51, 169.06, 159.75, 159.64, 152.44, 149.79, 132.69, 130.74, 129.18, 129.14, 128.29, 127.57, 126.76, 119.96, 108.88, 106.11, 102.90, 101.28, 71.50, 62.05, 60.89, 56.22, 55.92, 29.81, 14.01, 13.95; HRMS-ESI calcd for $C_{26}H_{26}O_8$ $(M+Na)^+$ 489.15216, found 489.15199.

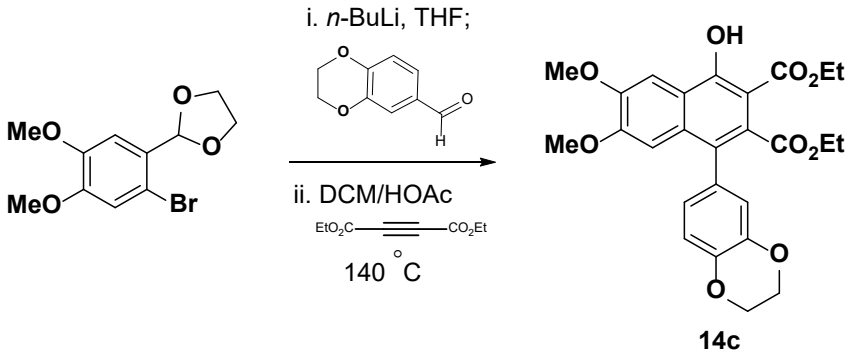

Dioxane 14c. Using 2-(2-bromo-4,5-dimethoxyphenyl)-1,3-dioxalane as the starting material (0.300 g, 1.040 mmol) and 2,3-dihydrobenzo[b][1,4]dioxine-6-carbaldehyde as the aldehyde (0.170 g, 1.040 mmol), the above general procedure afforded compound **14c** (0.105 g, 0.218 mmol, 21%) as a yellow oil: ^{1}H NMR (300 MHz, $CDCl_3$) δ 12.42 (s, 1H), 7.73 (s, 1H), 6.91 (d, *J*

= 8.2 Hz, 1H), 6.85 (d, *J* = 1.9 Hz, 1H), 6.80-6.76 (m, 2H), 4.39 (q, *J* = 7.2 Hz, 2H), 4.34-4.26 (m, 4H), 4.04 (s, 3H), 4.08 – 3.98 (m, 2H), 3.77 (s, 3H), 1.35 (t, *J* = 7.1 Hz, 3H), 1.05 (t, *J* = 7.1 Hz, 3H); ^{13}C NMR (400 MHz, $CDCl_3$) δ 170.49, 168.92, 159.71, 152.47, 149.81, 143.25, 143.20, 132.35, 130.34, 129.04, 127.65, 124.24, 119.99, 119.94, 116.90, 106.07, 102.88, 101.27, 64.60, 64.46, 62.07, 60.92, 56.21, 55.95, 14.01, 13.89; HRMS-ESI calcd for $C_{26}H_{26}O_9$ $(M+Na)^+$ 505.14710, found 505.14690.

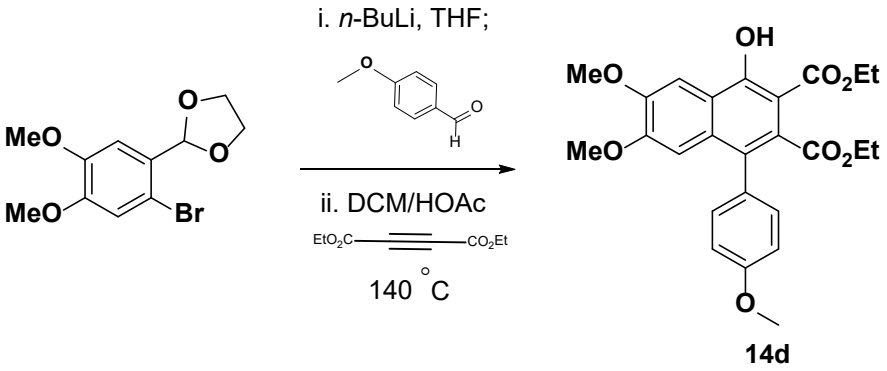

***p*-Anisaldehyde 14d.** Using 2-(2-bromo-4,5-dimethoxyphenyl)-1,3-dioxalane as the starting material (0.500 g, 1.729 mmol) and 4-methoxybenzaldehyde as the aldehyde (0.235 g, 1.729 mmol), the above general procedure afforded compound **14d** (0.128 g, 0.282 mmol, 16%) as a yellow oil: ^{1}H NMR (300 MHz, $CDCl_3$) δ 12.45 (s, 1H), 7.74 (s, 1H), 7.24 (d, *J* = 8.8 Hz, 2H), 6.97 (d, *J* = 8.7 Hz, 2H), 6.70 (s, 1H), 4.40 (q, *J* = 7.2 Hz, 2H), 4.05 (s, 3H), 3.97 (q, *J* = 7.1 Hz, 2H), 3.87 (s, 3H), 3.73 (s, 3H), 1.36 (t, *J* = 7.1 Hz, 3H), 0.99 (t, *J* = 7.2 Hz, 3H); ^{13}C NMR (400 MHz, $CDCl_3$) δ 170.52, 169.05, 159.72, 159.24, 152.48, 149.81, 132.59, 132.12, 129.42, 127.93, 119.97, 113.57, 106.04, 102.92, 101.29, 62.08, 60.94, 56.24, 55.88, 55.43, 14.03, 13.91; HRMS-ESI calcd for $C_{25}H_{26}O_8$ $(M+Na)^+$ 477.15207, found 477.15199.

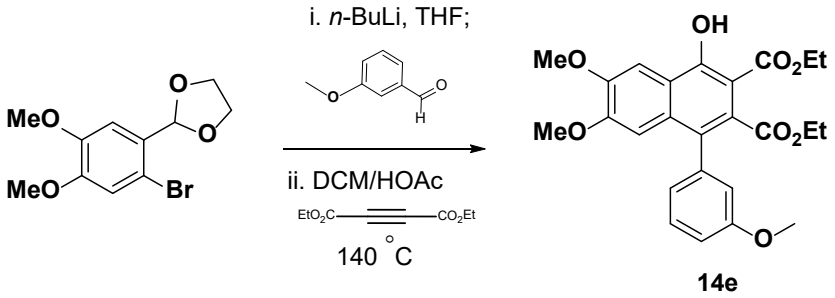

***m*-Anisaldehyde 14e.** Using 2-(2-bromo-4,5-dimethoxyphenyl)-1,3-dioxalane as the starting material (0.500 g, 1.729 mmol) and 3-methoxybenzaldehyde as the aldehyde (0.235 g, 1.729 mmol), the above general procedure afforded compound **14e** (0.112 g, 0.246 mmol, 14%) as a yellow oil solid: ^{1}H NMR (300 MHz, $CDCl_3$) δ 12.44 (s, 1H), 7.74 (s, 1H), 7.34 (dd, *J* = 9.9, 6.2 Hz, 1H), 6.99 – 6.85 (m, 3H), 6.74 (s, 1H), 4.40 (q, *J* = 7.2 Hz, 2H), 4.05 (s, 3H), 3.98 (q, *J* = 7.1 Hz, 2H), 3.81 (s, 3H), 3.73 (s, 3H), 1.36 (t, *J* = 7.2 Hz, 3H), 0.97 (t, *J* = 7.2 Hz, 3H); ^{13}C NMR (400 MHz, $(CD3)_2SO$) δ 169.78, 150.57, 149.75, 144.93, 142.89, 142.84, 129.54, 129.52, 128.13, 123.46, 123.42, 121.80, 119.35, 118.58, 116.56, 105.67, 100.83, 66.65, 64.23, 64.13, 55.68, 55.22; HRMS-ESI calcd for $C_{25}H_{26}O_8$ $(M+Na)^+$ 477.15213, found 477.15199.

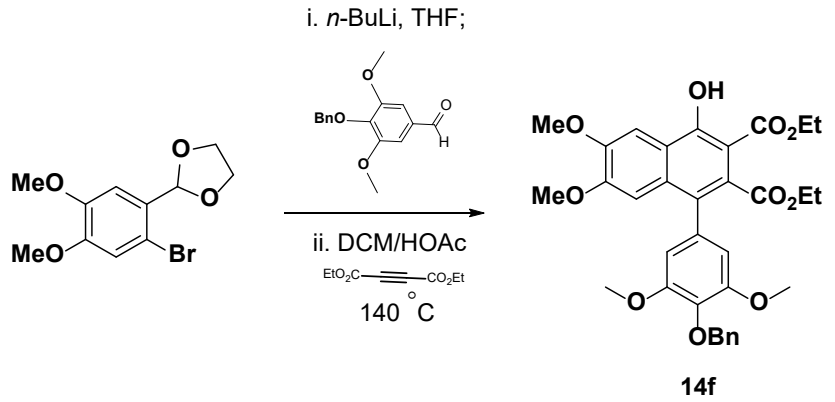

2-(benzyloxy)-1,3-dimethoxybenzene 14f. Using 2-(2-bromo-4,5-dimethoxyphenyl)-1,3-dioxalane as the starting material (0.500 g, 1.729 mmol) and 4-(benzyloxy)-3,5-dimethoxybenzaldehyde as the aldehyde (0.471 g, 1.729 mmol), the above general procedure afforded compound **14f** (0.110 g, 0.219 mmol, 13%) as a yellow solid: ^{1}H NMR (300 MHz, $CDCl_3$) δ 12.45 (s, 1H), 7.73 (s, 1H), 7.53 (d, *J* = 1.7 Hz, 1H), 7.50 (d, *J* = 1.3 Hz, 1H), 7.39 – 7.27 (m, 3H), 6.75 (s, 1H), 6.55 (s, 2H), 5.12 (s, 2H), 4.40 (q, *J* = 7.1 Hz, 2H), 4.04 (s, 3H), 3.98 (q, *J* = 7.1 Hz, 2H), 3.79 (s, 6H), 3.72 (s, 3H), 1.36 (t, *J* = 7.1 Hz, 4H), 0.98 (t, *J* = 7.1 Hz, 3H); ^{13}C NMR (400 MHz, $CDCl_3$) δ 170.39, 168.91, 159.78, 153.19, 152.53, 149.87, 137.85, 136.08, 132.74, 132.00, 128.68, 128.66, 128.19, 128.04, 127.97, 119.94, 108.26, 105.87, 102.88, 101.15, 74.99, 62.09, 61.01, 56.26, 56.21, 55.87, 13.99, 13.95

Note: Analogues **15a**, **15b**, **15c**, **15d**, and **15e** were first synthesized by Ms. Bernadette Latimer, a past undergraduate researcher in the Fuchs lab. I collected the characterization data.

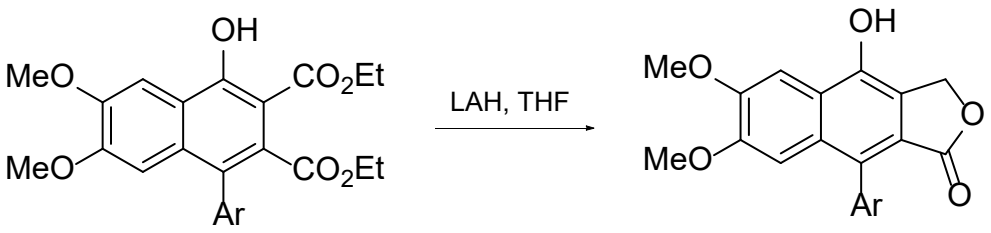

14a Ar = 2,2-difluorobenzo[d][1,3]dioxole
14b Ar = 2,3-dihydrobenzofuran
14c Ar = 2,3-dihydrobenzo[b][1,4]dioxine
14d Ar = 4-methoxyphenyl
14e Ar = 3-methoxyphenyl
14f Ar = 2-(benzyloxy)-1,3-dimethoxybenzene

15a Ar = 2,2-difluorobenzo[d][1,3]dioxole
15b Ar = 2,3-dihydrobenzofuran
15c Ar = 2,3-dihydrobenzo[b][1,4]dioxine
15d Ar = 4-methoxyphenyl
15e Ar = 3-methoxyphenyl
15f Ar = 2-(benzyloxy)-1,3-dimethoxybenzene

General procedure for lignan lactone formation:

To a solution of an arylnaphthalene diester dissolved in dry THF (1.00 equiv.) was added lithium aluminum hydride (4.00 equiv.) portion-wise at 0 °C. The reaction was warmed to 23 °C over 5 minutes prior to being cooled back down to 0 °C. It was then quenched dropwise with deionized water until the formation of gas was no longer observed. The pH of the reaction was then brought down to ~2 by dropwise addition of HCl (2M). The resulting aqueous mixture was then extracted with EtOAc. Combined organic layers were washed with brine then dried over anhydrous sodium sulfate and concentrated under reduced pressure. The crude solid was triturated with methanol to provide the corresponding products.

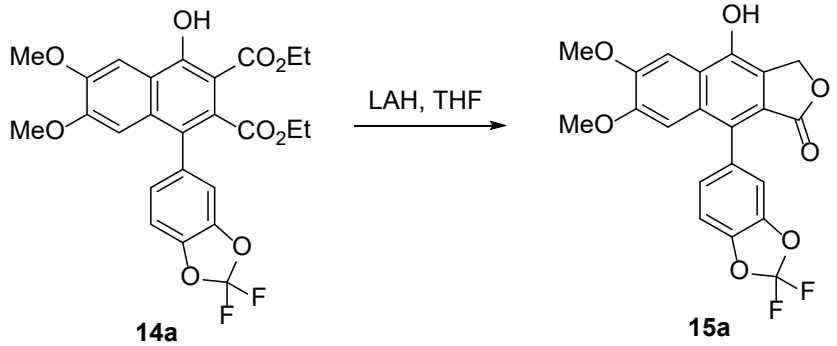

14a **15a**

Difluorobenzodioxole lactone 15a. Using difluorobenzodioxane **14a** (0.118 g, 0.234 mmol) as the starting material, the above general procedure afforded difluorobenzodioxole lactone **15a** (0.071 g, 0.171 mmol, 73%) as a pale pink solid: ^{1}H NMR (400 MHz, Acetone) δ 9.40 (s, 1H), 7.72 (s, 1H), 7.40 (d, *J* = 8.2 Hz, 1H), 7.30 (d, *J* = 1.2 Hz, 1H), 7.19 (dd, *J* = 8.2, 1.5 Hz, 1H), 7.02 (s, 1H), 5.39 (s, 2H), 4.01 (s, 3H), 3.73 (s, 3H); ^{13}C NMR (400 MHz, (CD3)2CO) δ 170.34, 152.28, 151.65, 146.24, 133.22, 130.86, 129.86, 127.45, 124.51, 122.75, 120.26, 113.28, 110.06, 106.38, 101.46, 67.23, 56.13, 55.79; HRMS-ESI calcd for $C_{21}H_{14}F_2O_7$ $(M+H)^+$ 417.07868, found 417.07804.

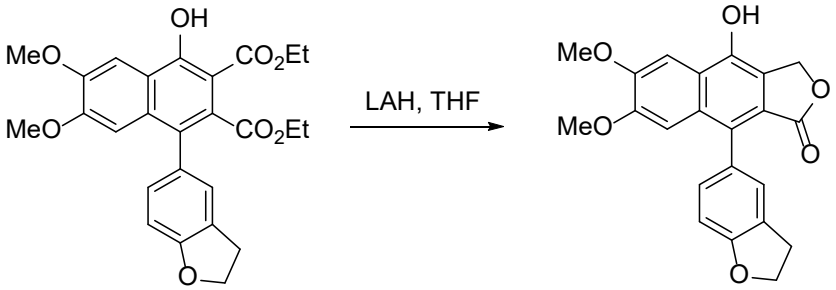

14b **15b**

Tetrahydrofuran lactone 15b. Using tetrahydrofuran **14b** (0.082 g, 0.176 mmol) as the starting material, the above general procedure afforded tetrahydrofuran lactone **15b** (0.039 g, 0.103 mmol, 59%) as a white powder: ^{1}H NMR (400 MHz, DMSO) δ 7.62 (s, 1H), 7.15 (s, 1H), 7.03 – 6.97 (m, 2H), 6.85 (d, *J* = 8.3 Hz, 1H), 5.35 (s, 2H), 4.61 (t, *J* = 8.6 Hz, 2H), 3.93 (s, 3H), 3.63 (s, 3H), 3.28 – 3.20 (m, 2H); ^{13}C NMR (400 MHz, DMSO) δ 170.10, 159.36, 150.67, 149.80, 144.82, 130.64, 130.25, 129.81, 127.50, 127.09, 127.00, 123.62, 121.97, 118.64, 108.50, 105.86, 100.92, 71.25, 66.75, 55.81, 55.32, 29.25; HRMS-ESI calcd for $C_{22}H_{18}O_6$ $(M+H)^+$ 379.11795, found 379.11761.

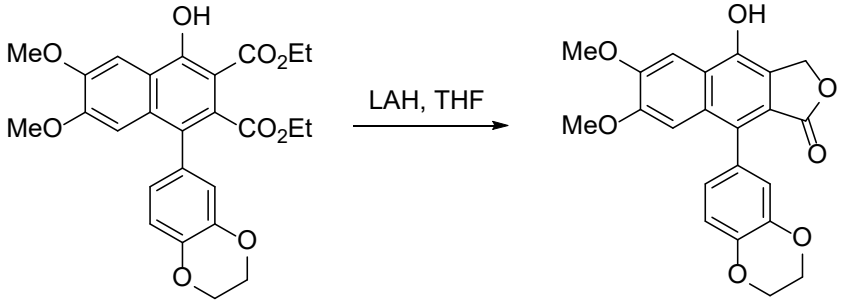

14c **15c**

Dioxane lactone 15c. Using dioxane **14c** (0.080 g, 0.166 mmol) as the starting material, the above general procedure afforded dioxane lactone **15c** (0.027 g, 0.068 mmol, 41%) as a white powder: ^{1}H NMR (400 MHz, DMSO) δ 10.37 (s, 1H), 7.62 (s, 1H), 6.97 – 6.92 (m, 2H), 6.79 – 6.73 (m, 2H), 5.35 (s, 2H), 4.31 (d, *J* = 3.8 Hz, 4H), 3.94 (s, 3H), 3.64 (s, 3H); ^{13}C NMR (400 MHz, DMSO) δ 169.79, 150.57, 149.76, 144.94, 142.89, 142.84, 129.52, 128.14, 123.46, 123.43, 121.81, 119.35, 118.58, 116.56, 105.67, 100.83, 66.66, 64.23, 64.13, 55.69, 55.22; HRMS-ESI calcd for $C_{22}H_{18}O_7$ $(M+H)^+$ 395.11296, found 395.11253.

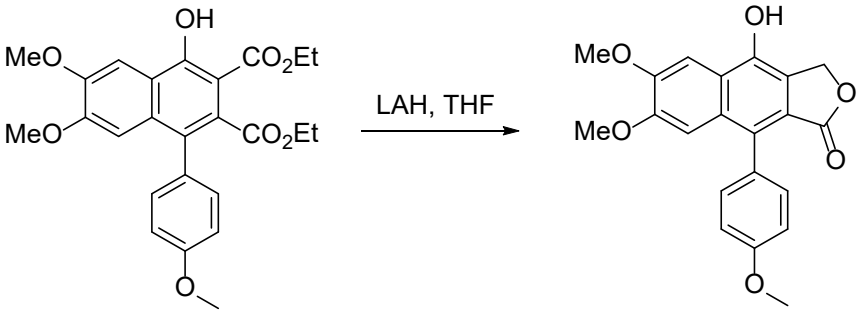

14d **15d**

***p*-Anisaldehyde lactone 15d.** Using *p*-anisaldehyde **14d** (0.370 g, 0.814 mmol) as the starting material, the above general procedure afforded *p*-anisaldehyde lactone **15d** (0.137 g, 0.374 mmol, 46%) as a white powder: ^{1}H NMR (300 MHz, DMSO) δ 7.65 (s, 1H), 7.27 – 7.20 (m,

2H), 7.07 – 7.01 (m, 2H), 6.95 (s, 1H), 5.37 (s, 2H), 3.95 (s, 3H), 3.85 (s, 3H), 3.63 (s, 3H); ^{13}C NMR (101 MHz, DMSO) δ 169.77, 158.58, 150.45, 149.64, 144.83, 131.67, 129.80, 129.50, 127.11, 123.38, 121.79, 118.52, 113.27, 105.53, 100.81, 66.58, 55.61, 55.06, 55.03; HRMS-ESI calcd for $C_{21}H_{18}O_6$ $(M+H)^+$ 367.11777, found 367.11761.

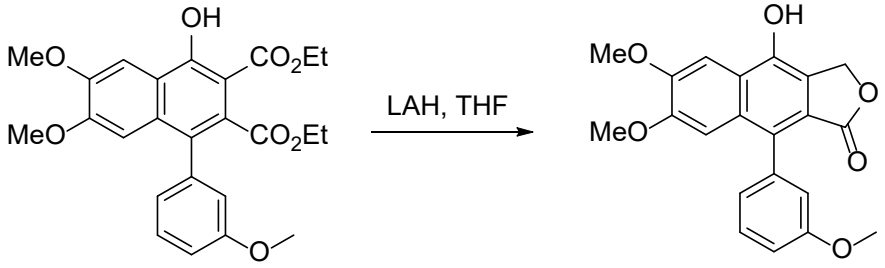

14e **15e**

***m*-Anisaldehyde lactone 15e.** Using *m*-anisaldehyde **14e** (0.250 g, 0.550 mmol) as the starting material, the above general procedure afforded *m*-anisaldehyde lactone **15e** (0.105 g, 0.287 mmol, 52%) as a white powder: ^{1}H NMR (300 MHz, DMSO) δ 10.41 (s, 1H), 7.63 (s, 1H), 7.39 (t, J = 7.9 Hz, 1H), 7.04 – 6.97 (m, 1H), 6.91 – 6.82 (m, 3H), 5.36 (s, 2H), 3.93 (s, 3H), 3.76 (s, 3H), 3.60 (s, 3H); ^{13}C NMR (400 MHz, DMSO) δ 169.56, 158.74, 150.50, 149.71, 145.01, 136.64, 129.17, 128.86, 123.27, 122.70, 121.69, 118.49, 116.02, 113.15, 105.44, 100.75, 66.64, 55.62, 55.04; HRMS-ESI calcd for $C_{21}H_{18}O_6$ $(M+H)^+$ 367.11777, found 367.11761.

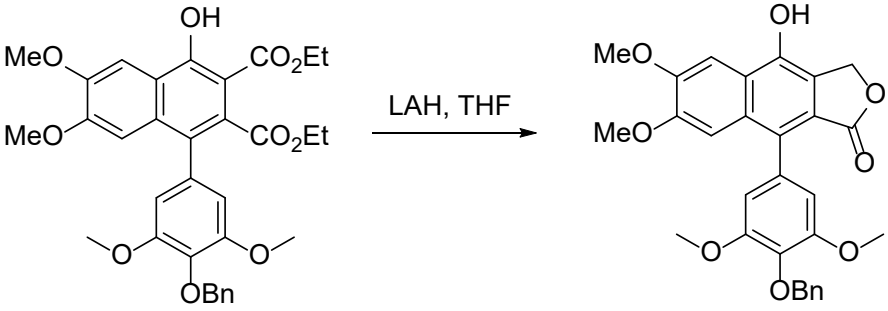

14f **15f**

2-(benzyloxy)-1,3-dimethoxybenzene lactone 15f. Using 2-(benzyloxy)-1,3-dimethoxybenzene **14f** (0.100 g, 0.199 mmol) as the starting material, the above general procedure afforded 2-(benzyloxy)-1,3-dimethoxybenzene lactone **15f** (0.010 g, 0.020 mmol, 10%) as an off-white powder: ^{1}H NMR (400 MHz, (CD3)2CO) δ 9.28 (s, 1H), 7.70 (s, 1H), 7.60 – 7.54 (m, 2H), 7.37 (tt, *J* = 8.1, 1.7 Hz, 2H), 7.33 – 7.28 (m, 1H), 7.13 (s, 1H), 6.67 (s, 2H), 5.38 (s, 2H), 5.09 (s, 2H), 4.00 (s, 3H), 3.82 (s, 6H), 3.72 (s, 3H); ^{13}C NMR (400 MHz, (CD3)2CO) δ 170.17, 154.15, 152.21, 151.29, 145.64, 139.56, 137.45, 132.18, 132.08, 130.95, 128.98, 128.86, 128.38, 124.47, 122.80, 119.72, 109.24, 107.02, 101.29, 75.11, 66.96, 56.59, 56.12, 55.80; HRMS-ESI calcd for $C_{29}H_{26}O_8$ $(M+H)^+$ 503.17023, found 503.17004.

References

[1] CDC - Basic Information About Ovarian Cancer. (n.d.). Retrieved from https://www.cdc.gov/cancer/ovarian/basic_info/index.htm

[2] Barnum, K. J., & O'Connell, M. J. (2014). Cell cycle regulation by checkpoints. *Methods in molecular biology (Clifton, N.J.)*, *1170*, 29-40.

[3] Genetics. (n.d.). Retrieved from https://www.cancer.gov/about-cancer/causes-prevention/genetics

[4] Signs and Symptoms of Ovarian Cancer. (n.d.). Retrieved from https://www.cancer.org/cancer/ovarian-cancer/detection-diagnosis-staging/signs-and-symptoms.html

[5] Charlton, J. L., Oleschuk, C. J., & Chee, G.-L. (January 01, 1996). Hindered rotation in arylnaphthalene lignans. *Journal of Organic Chemistry, 61,* 10.)USCS Data Visualizations. (n.d.). Retrieved from https://gis.cdc.gov/Cancer/USCS/DataViz.html

[6] USCS Data Visualizations. (n.d.). Retrieved from https://gis.cdc.gov/Cancer/USCS/DataViz.html

[7] WHO - Cancer. (n.d.). Retrieved from https://www.who.int/en/news-room/fact-sheets/detail/cancer

[8] Martin, L. P., & Schilder, R. J. (January 01, 2009). Management of recurrent ovarian carcinoma: current status and future directions. *Seminars in Oncology, 36,* 2, 112-25.

[9] Korkmaz, T., Seber, S., & Basaran, G. (February 01, 2016). Review of the current role of

targeted therapies as maintenance therapies in first and second line treatment of epithelial ovarian cancer; In the light of completed trials. *Critical Reviews in Oncology / Hematology, 98,* 180-188.

[10] Horwitz, S. B. (January 01, 1992). Mechanism of action of taxol. *Trends in Pharmacological Sciences, 13,* 4, 134-6.

[11] Jubin, T., Kadam, A., Jariwala, M., Bhatt, S., Sutariya, S., Gani, A. R., Gautam, S., ... Begum, R. (August 01, 2016). The PARP family: insights into functional aspects of poly (ADP-ribose) polymerase-1 in cell growth and survival. *Cell Proliferation, 49,* 4, 421-437.

[12] Cytotoxic-chemotherapy-mechanisms-of-action - My Cancer Genome. (n.d.). Retrieved from https://www.mycancergenome.org/content/molecular-medicine/pathways/cytotoxic-chemotherapy-mechanisms-of-action

[13] Vasilev, N., Elfahmi, N. V., Bos, R., Kayser, O., Momekov, G., Konstantinov, S., & Ionkova, I. (January 01, 2006). Production of justicidin B, a cytotoxic arylnaphthalene lignan from genetically transformed root cultures of Linum leonii. *Journal of Natural Products, 69,* 7, 1014-1017.

[14] Tuchinda, P., Kornsakulkarn, J., Pohmakotr, M., Kongsaeree, P., Prabpai, S., Yoosook, C., Kasisit, J., ... Reutrakul, V. (January 01, 2008). Dichapetalin-type triterpenoids and lignans from the aerial parts of Phyllanthus acutissima. *Journal of Natural Products, 71,* 4, 655-63.

[15] Unander, D. W., Webster, G. L., & Blumberg, B. S. (January 01, 1995). Usage and bioassays in Phyllanthus (Euphorbiaceae). IV. Clustering of antiviral uses and other effects. *Journal of Ethnopharmacology, 45,* 1, 1-18.

[16] Ren, Y., Lantvit, D. D., Deng, Y., Kanagasabai, R., Gallucci, J. C., Ninh, T. N., Chai, H. B., ... Kinghorn, A. D. (January 01, 2014). Potent cytotoxic arylnaphthalene lignan lactones from Phyllanthus poilanei. *Journal of Natural Products, 77,* 6, 1494-504.

[17] Shi, D. K., Zhang, W., Ding, N., Li, M., & Li, Y. X. (January 01, 2012). Design, synthesis and biological evaluation of novel glycosylated diphyllin derivatives as topoisomerase II inhibitors. *European Journal of Medicinal Chemistry, 47,* 1, 424-31.

[18] Zhao, Y., Ni, C., Zhang, Y., & Zhu, L. (August 01, 2012). Synthesis and Bioevaluation of Diphyllin Glycosides as Novel Anticancer Agents. *Archiv Der Pharmazie, 345,* 8, 622-628.

[19] Gui, M., Shi, D.-K., Huang, M., Zhao, Y., Sun, Q.-M., Zhang, J., Chen, Q., ... Ding, J. (October 01, 2011). D11, a novel glycosylated diphyllin derivative, exhibits potent anticancer activity by targeting topoisomerase IIα. *Investigational New Drugs : the Journal of New Anticancer Agents, 29,* 5, 800-810.

[21] Woodard, J. L., Huntsman, A. C., Patel, P. A., Chai, H. B., Kanagasabai, R., Karmahapatra, S., Young, A. N., ... Fuchs, J. R. (January 01, 2018). Synthesis and antiproliferative activity of derivatives of the phyllanthusmin class of arylnaphthalene lignan lactones. *Bioorganic & Medicinal Chemistry, 26,* 9, 2354-2364.

[22] Young, A. N., Herrera, D., Huntsman, A. C., Korkmaz, M. A., Lantvit, D. D., Mazumder, S., Kolli, S., ... Burdette, J. E. (January 01, 2018). Phyllanthusmin Derivatives Induce Apoptosis and Reduce Tumor Burden in High-Grade Serous Ovarian Cancer by Late-Stage Autophagy Inhibition. *Molecular Cancer Therapeutics, 17,* 10, 2123-2135.

[23] Ju, L. L., Zhao, C. Y., Ye, K. F., Yang, H., & Zhang, J. (January 01, 2016). Expression

and clinical implication of Beclin1, HMGB1, p62, survivin, BRCA1 and ERCC1 in epithelial ovarian tumor tissues. *European Review for Medical and Pharmacological Sciences, 20,* 10, 1993-2003

[24] Spowart, J. E., Townsend, K. N., West, N. R., Ries, J. N., Watson, P. H., Lum, J. J., West, N. R., ... Lum, J. J. (January 01, 2012). The autophagy protein LC3A correlates with hypoxia and is a prognostic marker of patient survival in clear cell ovarian cancer. *Journal of Pathology, 228,* 4, 437-447.

[25] Boucher, M. M., Furigay, M. H., Quach, P. K., & Brindle, C. S. (July 21, 2017). Liquid–Liquid Extraction Protocol for the Removal of Aldehydes and Highly Reactive Ketones from Mixtures. *Organic Process Research & Development.*

[26] Epsztajn, J., Jozwiak, A., & Szczesniak, A. K. (August 21, 1998). Application of organolithium and related reagents in synthesis. Part 21.1 Synthetic strategies based on ortho-aromatic metallation. A concise regiospecific synthesis of arylnaphthalanes as precursors of naphthylisoquinoline alkaloids. *Perkin Transactions 1, 1998,* 16, 2563.

Appendix: Characterization Data of Selected Compounds

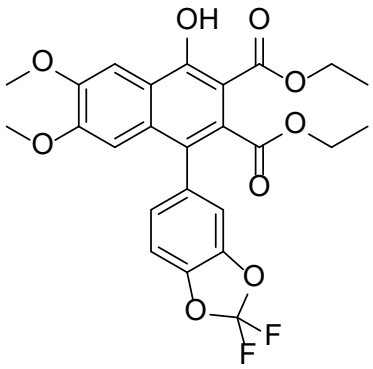

^{1}H NMR (300 MHz, $CDCl_3$)

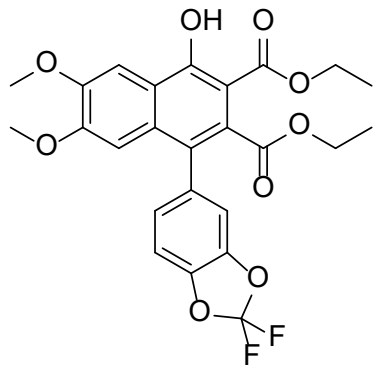

^{13}C NMR (400 MHz, $CDCl_3$)

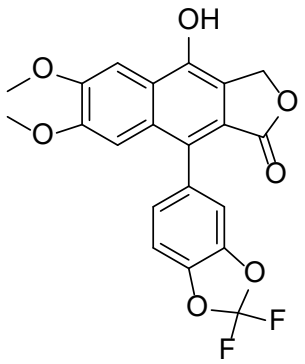

^{1}H NMR (300 MHz, $(CD3)_2CO$)

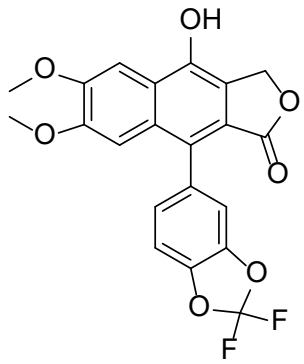

^{13}C NMR (400 MHz, $(CD3)_2CO$)

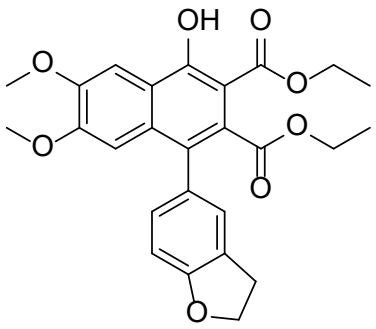

^{1}H NMR (300 MHz, $CDCl_3$)

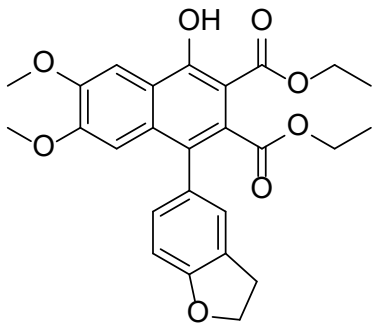

^{13}C NMR (400 MHz, $CDCl_3$)

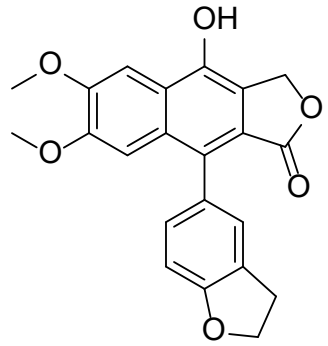

^{1}H NMR (400 MHz, $CDCl_3$)

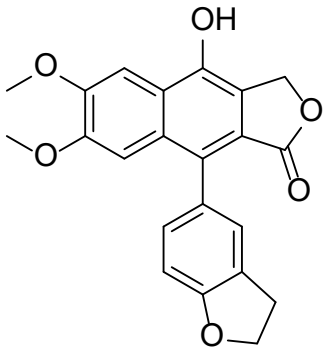

^{13}C NMR (400 MHz, $CDCl_3$)

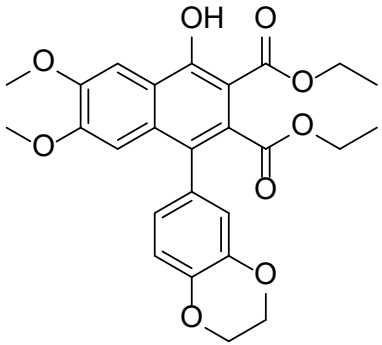

^{1}H NMR (300 MHz, $CDCl_3$)

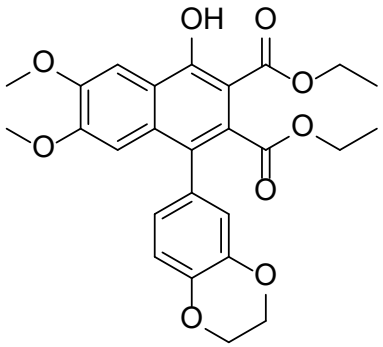

^{13}C NMR (400 MHz, $CDCl_3$)

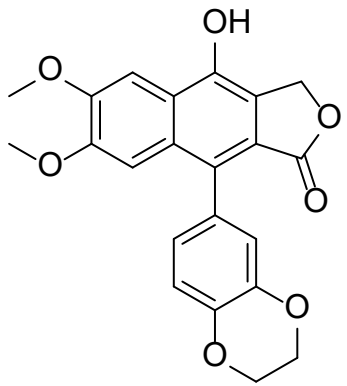

^{1}H NMR (400 MHz, $(CD3)_2SO$)

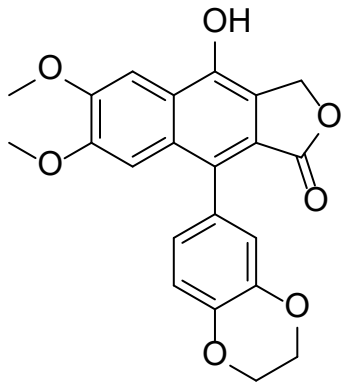

^{13}C NMR (400 MHz, $(CD3)_2SO$)

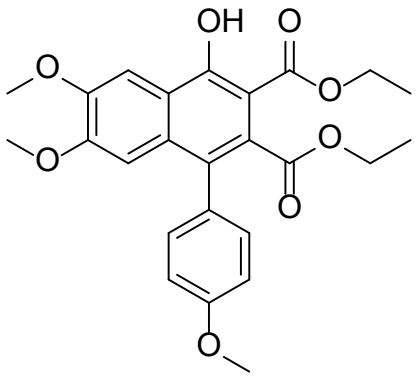

^{1}H NMR (300 MHz, $CDCl_3$)

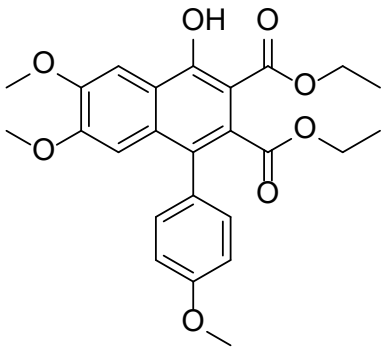

^{13}C NMR (400 MHz, $CDCl_3$)

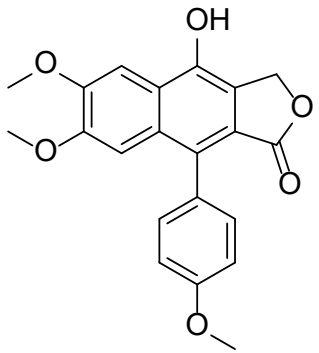

^{1}H NMR (300 MHz, $(CD3)_2SO$)

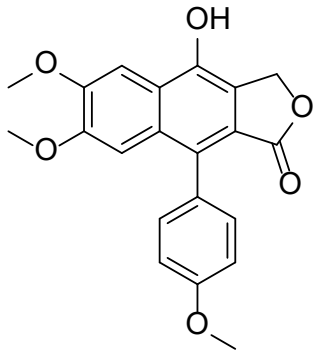

^{13}C NMR (400 MHz, $(CD3)_2SO$)

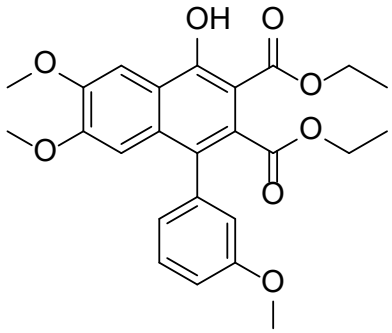

^{1}H NMR (300 MHz, $CDCl_3$)

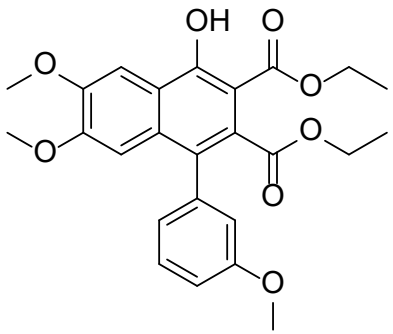

^{13}C NMR (400 MHz, $(CD3)_2SO$)

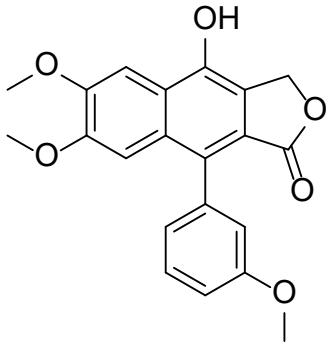

^{1}H NMR (300 MHz, $(CD3)_2SO$)

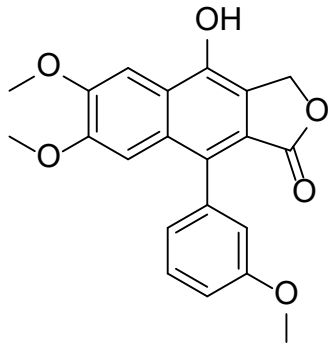

^{13}C NMR (400 MHz, $(CD3)_2SO$)

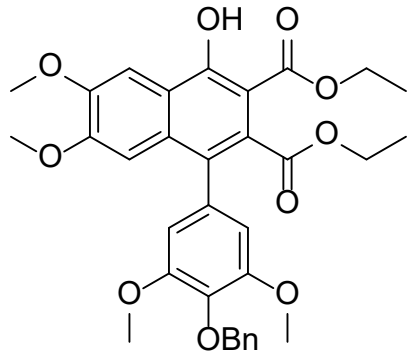

^{1}H NMR (300 MHz, $CDCl_3$)

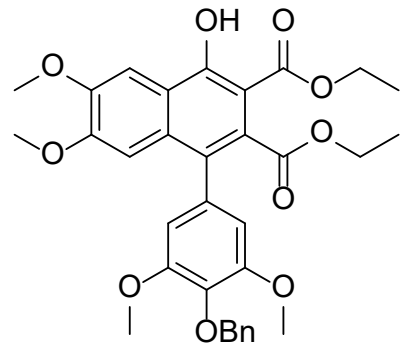

^{13}C NMR (400 MHz, $CDCl_3$)

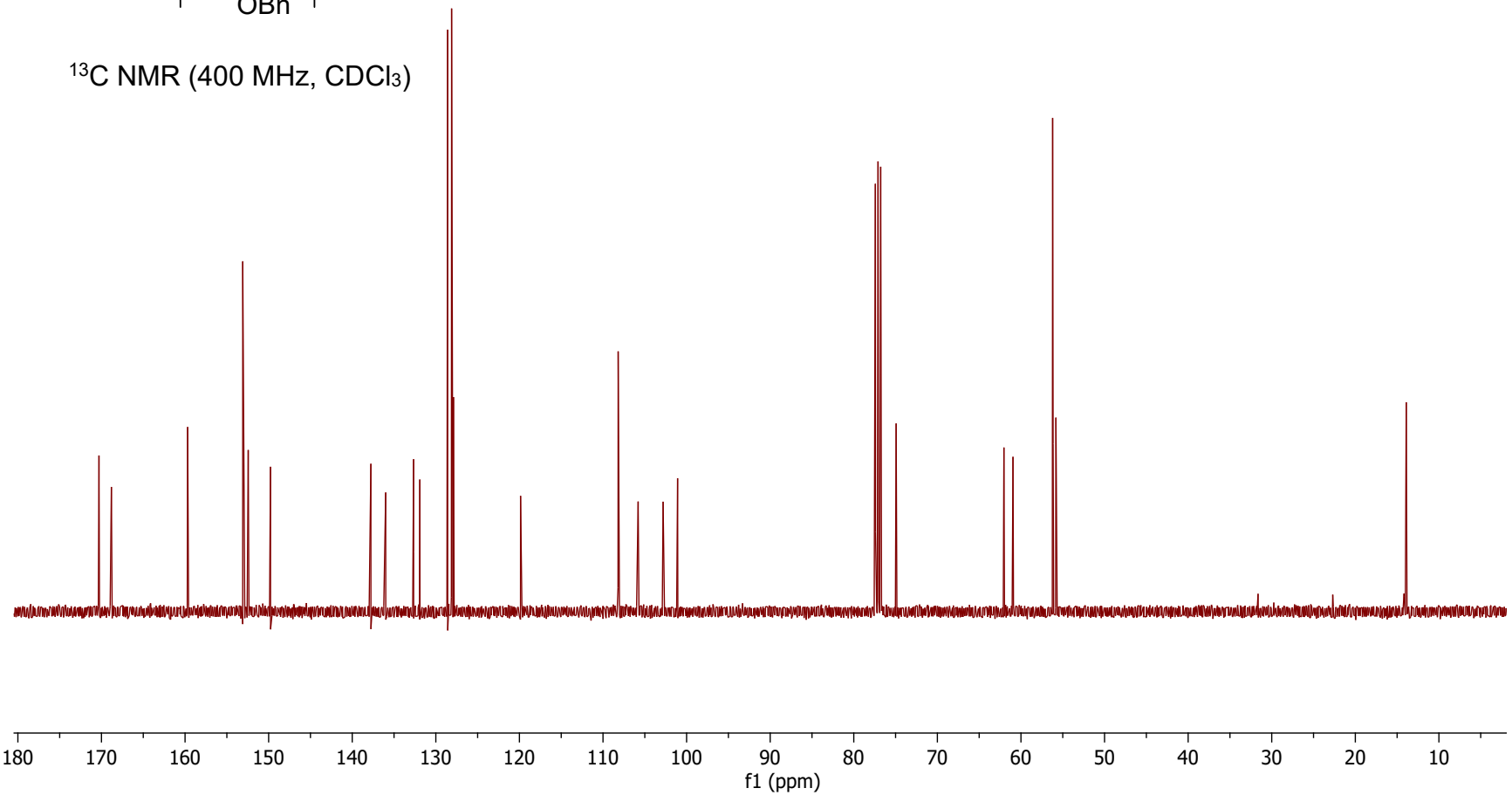

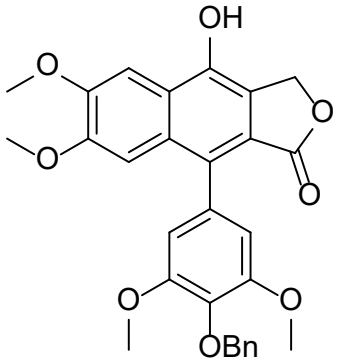

^{1}H NMR (400 MHz, $(CD3)_2CO$)

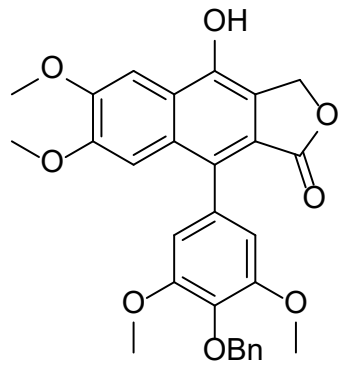

^{13}C NMR (400 MHz, $(CD3)_2CO$)